Engineering Science and Technology, an International Journal xxx (xxxx) xxx

HOSTED BY

ELSEVIER

Contents lists available at ScienceDirect

Engineering Science and Technology, an International Journal

journal homepage: www.elsevier.com/locate/jestch

Full Length Article

An investigation on optimum grinding system and conditions for steel plant ARP by-product α-Fe_2O_3 for pigment industry

Ozgur Karakas [a,*], Erdogan Kanca [b]

[a] MMK Metalurji San. Tic. ve Liman İşl. A.Ş., Özerli Mah. Alparslan Türkeş Blv., No: 342/98, Hatay 31600, Turkey
[b] Department of Mechanical Engineering, Iskenderun Technical University, Hatay 31200, Turkey

ARTICLE INFO

Article history:
Received 5 December 2019
Revised 21 February 2020
Accepted 11 March 2020
Available online xxxx

Keyword:
Iron and steel
α-Fe_2O_3
Red iron oxide pigment
Dry grinding
Jet mill

ABSTRACT

After some other processes, α-Fe_2O_3 red powder particles -by-product of regeneration of spent pickling liquor in ARP in iron and steel industry- should be ground up to pigment grade to convert it to a value added product, red iron oxide pigment. In this study, grinding tests on α-Fe_2O_3 red powder were performed using four different types of laboratory-scale mills, namely the vibrating cup mill, vertical ball mill, planetary ball mill, and fluidized bed jet mill. The particle structure of the α-Fe_2O_3 was investigated by SEM, while its chemical composition was determined by ICP-OES, density, LOI, humidity, Cl content etc. were determined by laboratory tests. Particle size distribution and surface area value of each ground sample was determined using the laser diffraction method. Targeted particle size distribution ranges could only be achieved with the jet mill. Other mills encountered caking and adhesion problem with α- Fe_2O_3. It was assessed that the adhesion to the inner walls of the grinding chamber and the caking effect were both caused by the humidity content of the material. The grinding yield of the material was found to increase with increased jet mill grinding air pressure (0.8, 3.2 and 7 bars).

1. Introduction

In the steel industry, the scales on the surface of the hot-rolled steel are removed using a variety of acidic solutions. The most commonly used acid for this purpose is hydrochloric acid (HCl). The acid solution used for removal of the scales gets polluted with the iron that dissolves inside it, and the concentration of HCl decreases over time. The chloride ions within this waste acid solution are protonated at acid regeneration plants (ARP) and are recovered as the pure hydrochloric acid, with a concentration varying between 18 and 20%. During this process, iron ions are oxidized to α-Fe_2O_3 red powder, and are collected at the bottom of the reactor as a by-product [1–3].

Steel producers tend to sell α-Fe_2O_3 red powder at a relatively low price as a raw material to other companies that produce ferrite [4,5]. Steel production companies can add this by-product to the sintering process as an additional iron source, and obtain a small amount of added value [6]. The companies which have α-Fe_2O_3 red powder may sell it or use it in their sintering facilities, but in both cases, their aim is to get rid of the α-Fe_2O_3 red powder in a useful manner. Indeed, even a mid-sized pickling facility can produce up to 5,000 tons of α-Fe_2O_3 red powder annually. When produced as a by-product in this manner, α-Fe_2O_3 red powder has a low bulk density at approximately 0.5–0.6 ton/m^3, and a closed storage area of approximately 15,000 m^2 would be required to store 5000 tons of α-Fe_2O_3 red powder. If unsolved, it is evident that this storage problem will grow out of proportions. For this reason, steel producers with excessive amounts of α-Fe_2O_3 red powder often have to give it away for free [7].

Many studies are being conducted to investigate how the added value obtained from the use of α-Fe_2O_3 red powder can be increased, instead of selling it for ferrite production or using it as a sintering raw material.

Ferreire and Mansur (2011) conducted a statistical analysis on the operating parameters used in the regeneration of the waste acid from a picking line that employed hydrochloric acid in order to find the parameters that affected the quality of the α-Fe_2O_3 red powder produced as a by-product. They examined the effect of the reactor temperature of the acid regeneration plant, waste acid supply rate and pressure, and supply air-blister gas (coke oven gas) mixture rates on the quality characteristics of α-Fe_2O_3 red powder (such Cl, Fe, Si, and H_20 content). The researchers demonstrated that the most important parameters that affected the ratio of these components were the reactor temperature and the solution supply rate [8].

* Corresponding author.
E-mail address: ozgurkarakas06@gmail.com (O. Karakas).
Peer review under responsibility of Karabuk University.

https://doi.org/10.1016/j.jestch.2020.03.005
2215-0986/

Inoue and Suito (1990) worked on the purification of the α-Fe_2O_3 red powder from an acid regeneration plant of a steel producer using the glass-ceramic method. They obtained high-purity α-Fe_2O_3 red powder from the flax treated with diluted HCl after being sintered with the mixture of Na_2O and B_2O_3 [9].

A recent venue of study is to obtain Fe^0 (metallic iron) powder by reducing the α-Fe_2O_3 red powder obtained from the acid regeneration plants. Cho et al. (2013), described this method, characterizing the metallic iron obtained with this method [10].

In recent years some studies focused on making this by-product suitable for use as a coloring pigment in paints, inks, plastics and construction chemicals, a method which would produce higher added value than the alternatives [11,12].

Ismail et al. (1992) managed to obtain red iron oxide pigments from the waste acid solution coming from the pickling line of a steel plant working with H_2SO_4. In this method, the waste acid - which is rich in $FeSO_4{\cdot}7H_2O$- is subjected to dry O_2 atmosphere at 700 °C for five hours. Moreover, the researchers also studied on the color saturation and hiding power of the red iron oxide pigment obtained [13].

Tang et al. (2016), produced nano-sized α-Fe_2O_3 using the precipitation method. They also examined the effect of the reaction temperature, mixing rate, and calcination temperature on the size of the primary particle size of the α-Fe_2O_3 produced. They measured the average primary particle size as 31.3 nm [14].

Kladnig (2004) conducted a comprehensive study on obtaining Red Iron Oxide (Pigment Red 101) from the waste hydrochloric acid solutions coming from the pickling lines at steel production plants using the "spray roasting" method. Kladnig also provided detailed information on the iron oxide pigment markets around the world and noted that the red iron oxide pigment consumption constituted more than half of the total iron oxide consumption. Kladnig talked about the spray roasting technology, reactor equipment, and process parameters, noting that the morphology and primary particle size of the red iron oxide were decisive on the color tone and strength. Noting that the red iron oxide pigment produced with this method should be ground, Kladnig pointed out that the material had surface area of approximately 3–4.5 m^2/g when removed from the reactor and using proper grinding systems this value could be increased [11]. Any detail is not given regarding the proper grinding system and operating parameters and performance of this grinding system in the study.

The red iron oxide pigments placed on the markets around the world are produced from natural mines or through chemical synthesis [15,16]. Four different methods are used for chemical synthesis: Laux process, Penniman process, calcination, and precipitation [11]. The material obtained from these chemical synthesis has to go through grinding in order to have a specific particle size distribution to be used as pigments. In these conventional red iron oxide pigment production processes, vertical ball mills, planetary ball mills or jet mills are used to grind these materials up to pigment grade after synthesis [17–19]. Concerning the subject material of this study, α-Fe_2O_3 red powder that is produced as a by-product in the acid regeneration plants of steel producers, any investigation on grinding systems and grinding parameters to convert it to pigment is not encountered in the literature. Most of the studies focused on purification of this by-product.

The α-Fe_2O_3 red powder, produced as a by-product in the acid regeneration plants of steel producers, consists of particles with sizes (diameters) ranging between 0.2 μm and 1500 μm [20,7]. This study aims to characterize and then determine the method which allows for a high efficiency and quality for grinding the α-Fe_2O_3 red powder into red iron oxide pigment by testing the use of different types of grinders. The targeted grinding quality, represented by the particle size distribution, was determined as D_{10} 0.5–1 μm, D_{50} 1–2 μm, and D_{90} 3–7 μm, which are ranges that make the product suitable for use as paint and/or in plastic production [21].

2. Experimental method

2.1. Physical and chemical properties of α-Fe_2O_3 red powder

For all the tests and experiments carried out as part of the study, a total of 500 kg of α-Fe_2O_3 red powder, produced in a single batch (which was supplied by the ARP of MMK Metalurji's facilities in Dörtyol, Turkey) was used. The α-Fe_2O_3 red powder bulk was first mixed thoroughly to obtain a homogeneous test sample. The bulk image of the α-Fe_2O_3 red powder used for grinding taken using Canon DSLR EOS 60D is given in Fig. 1.

Rigaku Smartlab X-Ray Powder Diffractometer (XRD) was used for phase analyses of the material. 11 peaks were observed which all referring to α-Fe_2O_3. XRD patterns of the sample were matched with JCPDS data, 01-080-5405 and 01-080-2377 patterns. Any other phase structure of iron oxide was not found. XRD patterns of the sample is given in Fig. 2.

Chloride content of the sample was determined using Hach Lange DR5000 spectrophotometer. The samples were dissolved in hot HCl solution and their chemical compositions were measured using Agilent 5110 ICP-OES device. All the iron ions were expressed as Fe_2O_3 according to the XRD results, other physical properties and chemical composition were measured using the equipment and methods listed in Table 1.

2.2. Grinding mills used in this study

The laboratory models of four different type of mills were used for dry grinding trial processes of the material. The properties of the laboratory-scale mills used are given in Table 2.

2.3. Particle size distribution analyses

The particle-size distribution of the original α-Fe_2O_3 red powder was measured before beginning grinding trials and measurements done also after grinding with each mill. Laser diffraction method is traditionally used in determining the particle-size distribution in paints, inks, plastics, construction chemicals and other areas where red iron oxide pigments are used [22]. For this reason, this method was used for particle-size distribution analysis.

Malvern Panalytical Mastersizer 3000 laser diffraction particle-size analyzer was used for the measurement of the particle-size distribution. All measurements were made in an aqueous suspen-

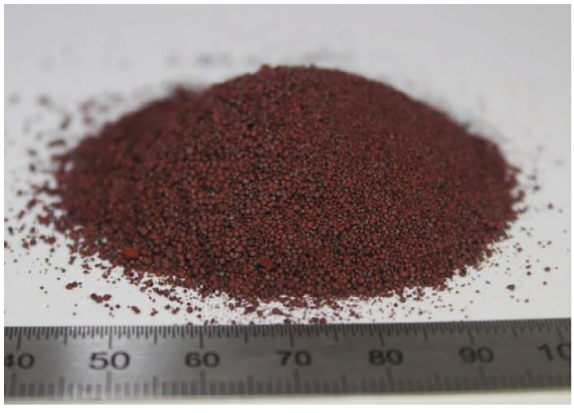

Fig. 1. Bulk image of the α-Fe_2O_3 red powder.

Please cite this article as: O. Karakas and E. Kanca, An investigation on optimum grinding system and conditions for steel plant ARP by-product α-Fe_2O_3 for pigment industry, Engineering Science and Technology, an International Journal, https://doi.org/10.1016/j.jestch.2020.03.005

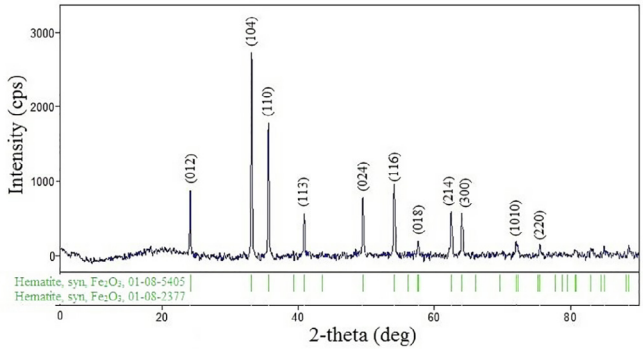

Fig. 2. XRD patterns of of the α-Fe_2O_3 red powder.

Table 1
Physical and chemical properties of the α-Fe_2O_3 red powder.

Property	Unit	Method	Value
α-Fe_2O_3	%	Titrimetric	98.5
MnO	%	ICP-OES	0.25
SiO_2	%	ICP-OES	0.15
Al_2O_3	%	ICP-OES	0.08
CaO	%	ICP-OES	0.01
MgO	%	ICP-OES	0.01
P_2O_5	%	ICP-OES	0.02
LOI (1000 °C)	%	Gravimetric	0.95
Cl^-	%	Spectrophotometric	0.37
Bulk Density	g/cm^3	Graduated Cylinder	0.51
Moisture Content (105 °C)	%	Gravimetric	1.08
pH (10% Suspension)	–	pH Meter	3.09

Table 2
Main properties of the laboratory-scale mills used.

Mill Type	Brand/Model	Speed Range	Grinder Reservoir Capacity
Vibrating cup mill	Fritsch/ PULVERISETTE 9	600–1500 rev/min	250 ml
Planetary ball mill	Retsch/Planetary Ball Mill PM 100	100–650 rev/min	500 ml
Vertical ball mill	JM-3I	100–1200	600 ml
Fluidized bed jet mill	NETZSCH/CGS 16	Max 12,000 rev/min classifier	210 mm Reservoir diameter

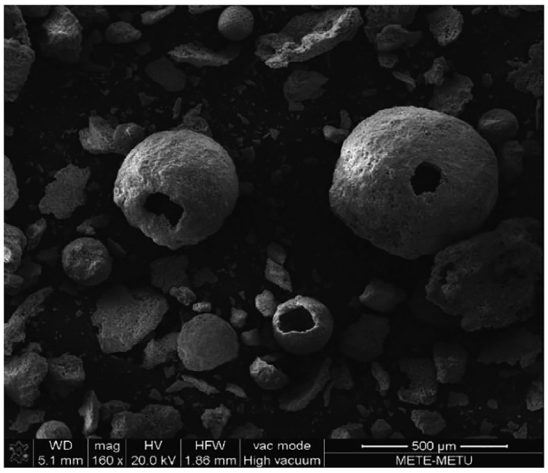

Fig. 3. SEM images of empty microspheres of the α-Fe_2O_3 red powder.

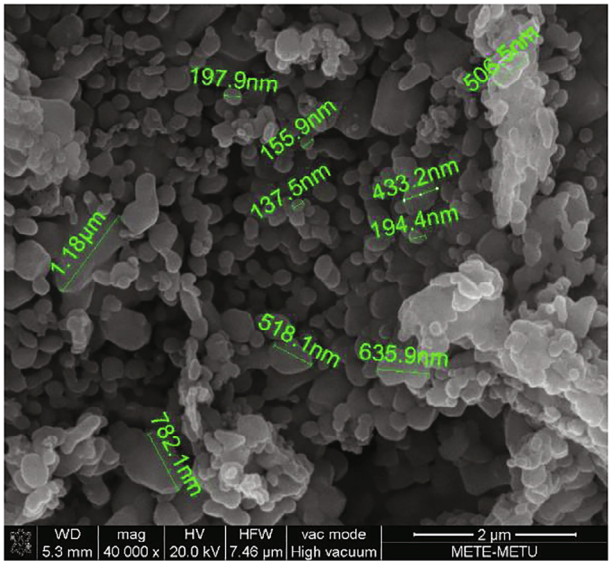

Fig. 4. SEM images of primary particles of the α-Fe_2O_3 red powder.

sion using the ultrasonic agitator, without the need for any additional wetting agent.

The studies on the morphology of the α-Fe_2O_3 red powder, produced as a by-product in the acid regeneration plants to be used as pigments, report the material to be in the form of hollow microspheres [11,23–25]. The images of the material taken before the grinding using QUANTA 400F Field Emission scanning electron microscope (SEM) were then studied to find out the structure of the hollow microspheres mentioned in the literature. The empty microspheres and the broken particles of these microspheres, and the primary particles of the material were then examined (Figs. 3 and 4).

Some pre-studies were run to find out optimum parameters for particle size distribution measurements. The pre-studies showed that applying ultrasonic agitation and increasing mixing speed result out a shifting on the particle size distribution curve to smaller side of the graph and cause an instability on measurements unlike grounded samples. It was concluded that the hollow microsphere particle shape of the unground samples shown in Fig. 2 have a tendency to crack down to smaller particles and using ultrasonic agitator and high mixing speeds during preparation of unground samples for particle-size distribution measurement would cause misleading results. Therefore, the ultrasonic agitator was not used and the mixing speed was kept at a low level for determining the particle size distribution measurement of unground materials. The parameters used in the particle-size distribution measurements made using the laser diffraction method are given in Table 3.

2.4. Particle size distribution analysis of α-Fe_2O_3 red powder before grinding

The particle size distribution measurements of the α-Fe_2O_3 red powder were taken both before grinding, and the measurement results are given in Table 4.

3. Grinding results and discussions

Following its physical, chemical and morphological characterization, the α-Fe_2O_3 red powder was ground to attain the targeted

Please cite this article as: O. Karakas and E. Kanca, An investigation on optimum grinding system and conditions for steel plant ARP by-product α-Fe_2O_3 for pigment industry, Engineering Science and Technology, an International Journal, https://doi.org/10.1016/j.jestch.2020.03.005

Table 3
Parameters for the laser diffraction particle size distribution measurements.

Sample	Dispersant	Refractive Index of the Dispersant	Ultra sound (%)	Mixing Rate (Rev/Min)	Refractive Index of α-Fe_2O_3	Laser Saturation (%)
Unground	Demineralized Water	1.33	None	300	2.98	8–12
Ground	Demineralized Water	1.33	10	2000	2.98	8–12

Table 4
The particle-size distribution of the α-Fe_2O_3 red powder before grinding.

D_{97} (μm)	D_{90} (μm)	D_{50} (μm)	D_{10} (μm)	Surface Area (m^2/g)
812.1	412.3	10.5	2.7	2.968

particle size using four different laboratory-scale mills. The grinding parameters of the equipment were differentiated depending on the laboratory conditions and the results of each grinding were visually inspected before the particle-size distribution and surface area were measured, and issues such as adhesion and caking were recorded.

3.1. Vibrating cup mill grinding

Samples, each weighing 100 g, were ground in the vibrating cup mill at five different speeds varying between 600 and 1400 rev/min, for three minutes each. High levels of adhesion to the cup walls and the caking of the α-Fe_2O_3 red powder were observed. The particle-size distribution was measured after each grinding run. The grinding parameters and measurement results are given in Table 5, while the images of the α-Fe_2O_3 red powder that adhered to the cup walls and caked are given in Fig. 5.

3.2. Vertical ball mill grinding

Samples, each weighing 100 g, were ground in the vertical ball mill using different grinding parameters. Adhesion to the cup walls and the caking of the α-Fe_2O_3 red powder at inner walls of the reservoir were observed. The particle-size distribution was measured after each grinding run. The grinding parameters and measurement results are given in Table 6, while the image showing the caking of the α-Fe_2O_3 red powder is given in Fig. 6.

3.3. Planetary ball mill grinding

Samples, each weighing 100 g, were ground in the planetary ball mill using different grinding parameters. Adhesion to the cup walls and the caking of the α-Fe_2O_3 red powder at ball surfaces were observed. The particle-size distribution was measured after each grinding run. The grinding parameters and measurement results are given in Table 7 while the image of the α-Fe_2O_3 red powder showing adhesion to ball surfaces and caking are given in Fig. 7.

Fig. 5. Intensive adhesion and caking at cup walls.

3.4. Fluidized bed jet mill grinding

The fluidized bed jet mill differed from the other types of mill used in this study as it offered continuous grinding process and it had the ability to select the part of the ground materials with desired particle size, using a classifier/sorter. The fluidized bed jet mill also differs in that it grinds materials by colliding the particles to be ground with each other and with the reservoir inner wall.

Due to these characteristics of the fluidized bed jet mill, the grinding trials were performed using three different grinding air pressures. In all grinding runs, the classifier's speed changed from lower to higher rates until the desired particle-size distribution could be obtained at each pressure value, which was then kept constant during each particular grinding process. When desired distribution ranges were obtained, a 30-minute grinding run was performed and the amount of the red powder iron oxide ground at the relevant pressure value was recorded and the hourly yield was calculated.

The grinding parameters used in the grinding runs with the fluidized bed jet mill and the particle size measurement values obtained at each run are given in Table 8.

Table 5
Measurement results after the vibrating cup mill grinding.

Speed rev/min	Caking	Time (min)	D_{97} (μm)	D_{90} (μm)	D_{50} (μm)	D_{10} (μm)	Surface Area (m^2/g)
600	Yes	3	201.6	98.5	7.2	2.1	3.345
800	Yes	3	189.6	92.8	8.8	2.2	3.261
1000	Yes	3	191.0	94.8	7.8	1.9	3.221
1200	Yes	3	180.5	90.9	7.1	2.0	3.310
1400	Yes	3	187.4	95.8	8.9	2.2	3.340
Average of measurements:			190.0	94.6	8.0	2.1	3.259

Please cite this article as: O. Karakas and E. Kanca, An investigation on optimum grinding system and conditions for steel plant ARP by-product α-Fe_2O_3 for pigment industry, Engineering Science and Technology, an International Journal, https://doi.org/10.1016/j.jestch.2020.03.005

Table 6
Measurement results after the vertical ball mill grinding.

Speed (rev/min)	1. Ball Size (mm)	1. Ball Amount (g)	2. Ball Size (mm)	2. Ball Amount (g)	Time (min)	Caking	D_{97} (μm)	D_{90} (μm)	D_{50} (μm)	D_{10} (μm)	Surface Area (m^2/g)
700	2.97	4435	–	–	5	Yes	157.6	79.8	5.9	1.5	3.624
700	2.97	4435	8.49	336	5	Yes	165.2	78.1	4.3	1.4	3.597
400	2.97	4435	–	–	10	Yes	154.5	77.7	4.2	1.2	3.658
700	2.97	4435	–	–	10	Yes	158.6	69.8	4.1	1.1	3.789
1000	2.97	4435	–	–	10	Yes	149.0	69.8	3.9	1.1	3.800
400	2.97	4435	8.49	336	10	Yes	136.5	59.4	4.8	1.2	3.781
700	2.97	4435	8.49	336	10	Yes	132.8	66.5	5.1	1.1	3.799
1000	2.97	4435	8.49	336	10	Yes	138.4	62.7	4.4	1.2	3.823
Average of measurements:							149.1	70.5	4.6	1.2	3.734

Fig. 6. Caked material after the vertical ball mill grinding.

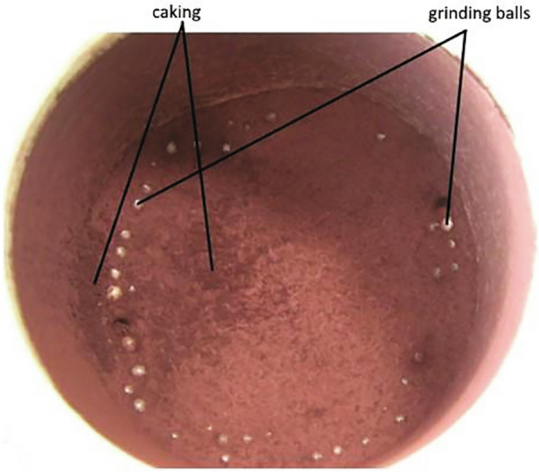

Fig. 7. Caked material after the planetary ball mill grinding.

3.5. Summary and discussion on grinding results

In the study conducted for grinding the α-Fe_2O_3 red powder to the pigment grade, the summary of the particle-size distribution results before grinding the material, the targeted values, and the values obtained after grinding with each mill, are given in Table 9.

Before grinding, 90% of the α-Fe_2O_3 red powder contained particles smaller than 412.3 μm, 50% smaller than 10.5 μm, and 10% smaller than 2.7 μm. During all the grinding tests it is targeted to change aforementioned distribution of the unground material to the ranges 3–7 μm, 1–2 μm and 0.5–1 μm, respectively, and an increase in the surface area of α-Fe_2O_3 red powder was also sought. This targeted distribution was obtained using the jet mill. In the trials conducted using the vibrating cup mill, vertical ball mill, and planetary ball mill, the targeted particle-size distribution values could not be reached.

With all the mills which failed to provide the targeted distribution values, it was observed that the α-Fe_2O_3 red powder adhered to the reservoir walls, cups, or partially to the balls, and the material was caked, which resulted in lower grinding performance. Some SEM images from caked material after milling are given in Fig. 8. This phenomenon of adhesion and caking is also observed during the grinding of other materials, particularly the foodstuff, depending on their structure. In the literature, the factors affecting the caking during the grinding process are listed as glass transition temperature, adhesion point temperature, and moisture content [26,27]. Given the moisture content of over 1%, it is believed that the basic factor for the adhesion and caking that decreased the grinding performance in the specified mill types for the grinding of the α-Fe_2O_3 red powder in our study was the moisture content.

Caking was not observed in any of the trials performed with the fluidized bed jet mill (none of three different grinding pressure settings), and all targeted particle-size distributions were reached. The present study indicated that the classifier speed should be lowered as the grinding pressure increases, so that the targeted distribution can be obtained and the amount ground per unit time

Table 7
Measurement results after the planetary ball mill grinding.

Speed (rev/min)	Ball Size (mm)	Ball Amount (g)	Time (min)	Caking	D_{97} (μm)	D_{90} (μm)	D_{50} (μm)	D_{10} (μm)	Surface Area (m^2/g)
200	5	500	5	Yes	197.6	91.6	5.1	1.5	3.692
400	5	500	5	Yes	175.4	86.1	6.0	1.4	3.620
600	5	500	5	Yes	164.0	82.3	5.3	1.2	3.785
200	3	620	5	Yes	168.3	88.9	5.8	1.1	3.501
400	3	620	5	Yes	159.6	79.8	5.0	1.1	3.499
600	3	620	5	Yes	126.5	88.1	6.0	1.2	3.622
Average of measurements:					165.2	86.1	5.5	1.3	3.620

Please cite this article as: O. Karakas and E. Kanca, An investigation on optimum grinding system and conditions for steel plant ARP by-product α-Fe_2O_3 for pigment industry, Engineering Science and Technology, an International Journal, https://doi.org/10.1016/j.jestch.2020.03.005

Table 8
Fluidized bed jet mill grinding parameters and measurement results.

Grinding No	Grinding Pressure (bar)	Classifier Speed (rev/min)	Time (min)	Grinding Yield (kg/hour)	Caking	D_{97} (μm)	D_{90} (μm)	D_{50} (μm)	D_{10} (μm)	Surface Area (m^2/g)
G1	0.8	2000	12	–	None	22.9	12.5	3.0	1.2	4.358
G2	0.8	3000	10	–	None	15.8	9.8	2.9	1.1	4.519
G3	0.8	4000	11	–	None	12.4	7.9	2.6	1.0	4.685
G4	0.8	5000	12	–	None	9.4	6.3	2.4	0.9	4.781
G5	0.8	6000	10	–	None	7.3	5.2	2.0	0.9	4.982
$G_{0.8}$	0.8	6000	30	6.3	None	6.9	5.1	1.9	0.8	5.024
G6	3.2	2000	10	–	None	18.1	11.3	2.4	1.0	4.521
G7	3.2	3000	10	–	None	12.1	7.9	2.2	0.9	4.671
G8	3.2	4000	11	–	None	9.0	6.2	1.9	0.9	4.802
G9	3.2	5000	10	–	None	7.0	5.7	1.8	0.9	4.958
$G_{3.2}$	3.2	5000	30	11.7	None	6.9	5.0	1.6	0.7	5.109
G10	7	2000	10	–	None	12.4	6.9	1.8	0.8	4.796
G11	7	3000	10	–	None	7.6	5.8	1.4	0.6	5.098
$G_{7.0}$	7	3000	30	23.5	None	7.5	5.5	1.4	0.6	5.168

Table 9
Summary of the grinding trials.

Grinding Trial	Caking	Yield (kg/hour)	D_{97} (μm)	D_{90} (μm)	D_{50} (μm)	D_{10} (μm)	Surface Area (m^2/g)
Unground α-Fe_2O_3	–	–	812.1	412.3	10.5	2.7	2.968
Vibrating cup mill	Yes	–	190.0	94.6	8.0	2.1	3.259
Vertical ball mill	Yes	–	149.1	70.5	4.6	1.2	3.734
Planetary ball mill	Yes	–	165.2	86.1	5.5	1.3	3.620
Jet Mill $G_{0.8}$	None	6.3	6.9	5.1	1.9	0.8	5.024
Jet Mill $G_{3.2}$	None	11.7	6.9	5.0	1.6	0.7	5.109
Jet Mill $G_{7.0}$	None	23.5	7.5	5.5	1.4	0.6	5.168
Grinding Target		–	–	3–7	1–2	0.5–1	–

can be increased. The average yields for three different pressures are given in Fig. 9.

On the other hand, the studies that will look for a solution to the problem of the decreasing grinding performance due to the caking in the vibration cup and ball mills may contribute to the efforts of increasing the added value of the α-Fe_2O_3 red powder, a by-product of the acid regeneration plants. The studies for optimizing the parameters, and undertaking the mathematical modeling of, the grinding with the fluidized jet mill will make similar contributions.

4. Conclusion

The efforts to obtain products with higher added value from the α-Fe_2O_3 red powder, which is produced as a by-product in the acid regeneration plants, is important particularly for the steel sector, and include the process of producing red iron oxide pigments from the red powder. This study focused on the physical, chemical and morphological characterization of the red powder, along with its grinding at the pigment grade.

Grinding trials were conducted using four different laboratory-scale mills, namely the vibrating cup mill, vertical ball mill, planetary ball mill, and fluidized jet mill. Before and after the grinding process, the particle-size distribution and surface area measurements of the red powder were performed using the laser diffraction method. SEM, ICP-OES, and other laboratory tests were used for the characterization of the red powder.

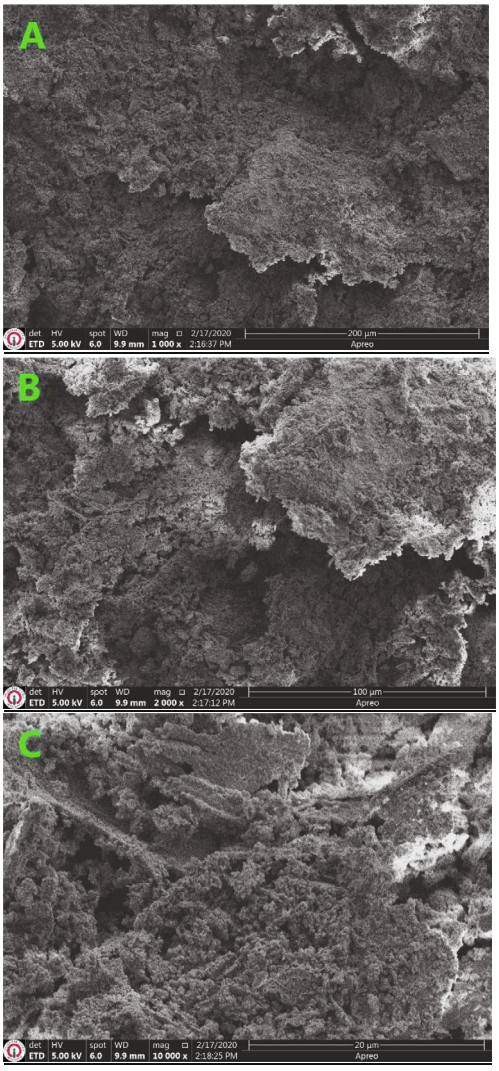

Fig. 8. A. ×1000 B. ×2000 and C. ×10k SEM images of caked α-Fe_2O_3 red powder.

With all mills, except the fluidized jet mill, adhesion to the reservoir walls and caking were observed, and the targeted particle-size distribution could not be achieved. It was concluded that the main factor for the caking was the high moisture content of the α-Fe_2O_3 red powder.

Please cite this article as: O. Karakas and E. Kanca, An investigation on optimum grinding system and conditions for steel plant ARP by-product α-Fe_2O_3 for pigment industry, Engineering Science and Technology, an International Journal, https://doi.org/10.1016/j.jestch.2020.03.005

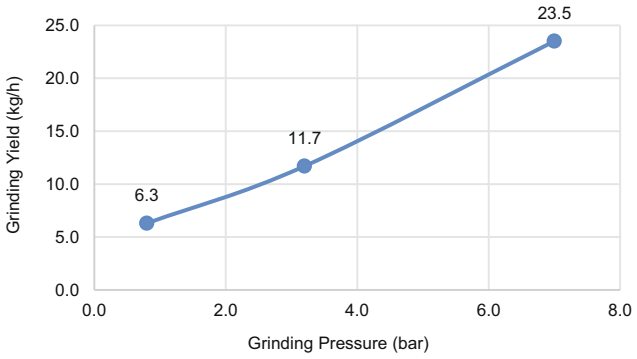

Fig. 9. Fluidized bed jet mill grinding pressure – grinding yield graph.

The targeted particle size was reached in all the trials performed with the jet mill with different grinding pressures (at 0.8, 3.2 and 7 bars), and the D_{90} value of the red powder before the grinding could be lowered from 412.3 μm down to 5.0 μm, while its surface area was increased from 2.968 m^2/g to 5.168 m^2/g. It was found that in the grinding runs made with jet mill, increasing the grinding air pressure resulted in an increased amount of ground material, and the amount of the material ground per hour at the grinding pressure of 7.0 bars was measured to be 23.5 kg.

Declaration of Competing Interest

The authors declare that they have no known competing financial interests or personal relationships that could have appeared to influence the work reported in this paper.

Acknowledgments

This study is supported by the Scientific and Technological Research Council of Turkey (TÜBİTAK, Project No. 3170019). We would like to express our thanks to MMK Metalurji CEO Mr. Denis Kvasov, who showed close interest in the project and allowed us to work on the pickling and acid regeneration lines and make use of the laboratory infrastructure of MMK Metalurji.

References

[1] Ö. Karakaş, Change in chloride content of regenerated red iron oxide particles in accordance with particle sizes.pdf, in: Mustafa Yaşar (Ed.), Proc. Third Int. Iron Steel Symp., Karabuk University Karabuk, Turkey, Karabük, 2017, pp. 239–243.

[2] L. Liu, P. Qi, Y. Liu, A review on spent pickling liquors treatment, DEStech Trans. Environ. Energy Earth Sci. (2017) 56–61, https://doi.org/10.12783/dteees/ese2017/14325.

[3] M. Regel-Rosocka, A review on methods of regeneration of spent pickling solutions from steel processing, J. Hazard. Mater. 177 (2010) 57–69, https://doi.org/10.1016/j.jhazmat.2009.12.043.

[4] M. Sugimoto, The past, present, and future of ferrites, J. Am. Ceram. Soc. 82 (2004) 269–280, https://doi.org/10.1111/j.1551-2916.1999.tb20058.x.

[5] L. Mei, A. Iizuka, E. Shibata, Recent progress on utilization of metal-rich wastes in ferrite processing: a review, Waste Biomass Valoriz. 9 (2018) 1669–1679, https://doi.org/10.1007/s12649-017-9909-x.

[6] W.F. Kladnig, A review of steel pickling and acid regeneration an environmental contribution, Int. J. Mater. Prod. Technol. 19 (2003) 550, https://doi.org/10.1504/IJMPT.2003.003471.

[7] N. Quaranta, M. Caligaris, H. López, M. Unsen, G. Pelozo, J. Pasquini, A. Cristóbal, Reuse of red powder of steel plants as fine addition in ceramic bricks manufacture, WIT Trans. Ecol. Environ. (2012) 1105–1113, https://doi.org/10.2495/SC120922.

[8] A.S. Ferreira, M.B. Mansur, Statistical analysis of the spray roasting operation for the production of high quality Fe2O3 from steel pickling liquors, Process Saf. Environ. Prot. 89 (2011) 172–178, https://doi.org/10.1016/j.psep.2010.11.005.

[9] R. Inoue, H. Suito, Purification of roasted iron oxide product from waste pickling liquor by glass-ceramic method, ISIJ Int. 30 (1990) 704–713, https://doi.org/10.2355/isijinternational.30.704.

[10] Y.I. Cho, B.H. Kim, S.J. Kim, J.J. Yun, H. Lee, S.H. Park, S.C. Jung, Preparation and characterization of zero valent iron powders via transfer type reductor using iron oxide from the acid regeneration process, Adv. Powder Technol. 24 (2013) 858–863, https://doi.org/10.1016/j.apt.2013.03.006.

[11] W.F. Kladnig, Synthetic Fe_2O_3 pigments derived by spray roasting hydrochloric solutions – a review, Int. J. Mater. Prod. Technol. 21 (2004) 555, https://doi.org/10.1504/IJMPT.2004.005628.

[12] N.E. Fouad, H.M. Ismail, M.I. Zaki, Recovery of red iron oxide pigmentary powders from chemically-modified steel-pickling chemical waste, J. Mater. Sci. Lett. 17 (1998) 27–29, https://doi.org/10.1023/A:1006533405891.

[13] H.M. Ismail, N.E. Fouad, M.I. Zaki, M.N. Magar, Particle characteristics of thermally recovered iron oxide pigments from steel-pickling chemical waste: Effects of heating variables, Powder Technol. 70 (1992) 183–188, https://doi.org/10.1016/0032-5910(92)85045-W.

[14] J. Tang, Y. Pei, Q. Hu, D. Pei, J. Xu, The recycling of ferric salt in steel pickling liquors: preparation of nano-sized iron oxide, Procedia Environ. Sci. 31 (2016) 778–784, https://doi.org/10.1016/j.proenv.2016.02.071.

[15] M.L. Franquelo, J.L. Perez-Rodriguez, A new approach to the determination of the synthetic or natural origin of red pigments through spectroscopic analysis, Spectrochim. Acta Part A Mol. Biomol. Spectrosc. 166 (2016) 103–111, https://doi.org/10.1016/j.saa.2016.04.054.

[16] I. Viera, A. Pérez-Gálvez, M. Roca, Green natural colorants, Molecules 24 (2019) 154, https://doi.org/10.3390/molecules24010154.

[17] E. Teke, M. Yekeler, U. Ulusoy, M. Canbazoglu, Kinetics of dry grinding of industrial minerals: calcite and barite, Int. J. Miner. Process. 67 (2002) 29–42, https://doi.org/10.1016/S0301-7516(02)00006-6.

[18] M. Ali, Transformation and powder characteristics of TiO2 during high energy milling, J. Ceram. Process. Res. 15 (2014) 290–293.

[19] L. Godet-Morand, A. Chamayou, J. Dodds, Talc grinding in an opposed air jet mill: start-up, product quality and production rate optimization, Powder Technol. 128 (2002) 306–313, https://doi.org/10.1016/S0032-5910(02)00172-9.

[20] A. Hosseini, Characterization and catalytic behaviour of nanostructured iron oxide powder from waste pickle liquor of steel industry, Int. J. ISSI. 7 (2010) 21–24. http://citeseerx.ist.psu.edu/viewdoc/download?doi=10.1.1.996.5488&rep=rep1&type=pdf.

[21] J.H. Braun, White Pigments, in: J. V. Koleske (Ed.), Paint Coat. Test. Man., 14th ed., ASTM International, Colombus, OH, USA, 2008: pp. 166–172.

[22] A. Rawle, The importance of particle sizing to the coatings industry Part 1: Particle size measurement, Adv. Colour Sci. Technol. 5 (2002) 1–12.

[23] S. Johansson, L.G. Westerberg, T.S. Lundström, Gas and particle flow in a spray roaster, J. Appl. Fluid Mech. 7 (2014) 187–196.

[24] W.F. Kladnig, New development of acid regeneration in steel pickling plants, J. Iron Steel Res. Int. 15 (2008) 1–6, https://doi.org/10.1016/S1006-706X(08)60134-X.

[25] M. Schiemann, S. Wirtz, V. Scherer, F. Bärhold, Spray roasting of iron chloride FeCl2: laboratory scale experiments and a model for numerical simulation, Powder Technol. 228 (2012) 301–308, https://doi.org/10.1016/j.powtec.2012.05.037.

[26] H. Jung, Y. Lee, W. Yoon, Effect of moisture content on the grinding process and powder properties in food: a review, Processes 6 (2018) 69, https://doi.org/10.3390/pr6060069.

[27] H. Mitra, H.A. Pushpadass, M.E.E. Franklin, R.P.K. Ambrose, C. Ghoroi, S.N. Battula, Influence of moisture content on the flow properties of basundi mix, Powder Technol. 312 (2017) 133–143, https://doi.org/10.1016/j.powtec.2017.02.039.